Magnetoelastic Coupling through the Antiferromagnet-to-Ferromagnet Transition of Quasi-Two-Dimensional $[Cu(HF_2)(pyz)_2]BF_4$ Using Infrared Spectroscopy

J. L. Musfeldt,[1] L. I. Vergara,[1] T. V. Brinzari,[1] C. Lee,[2] L. C. Tung,[3] J. Kang,[2] Y. J. Wang,[3] J. A. Schlueter,[4] J. L. Manson,[5] and M.-H. Whangbo[2]

[1]*Department of Chemistry, University of Tennessee, Knoxville, Tennessee 37996, USA*
[2]*Department of Chemistry, North Carolina State University, Raleigh, North Carolina 27695, USA*
[3]*National High Magnetic Field Laboratory, Tallahassee, Florida 32310, USA*
[4]*Materials Science Division, Argonne National Laboratory, Argonne, Illinois 60439, USA*
[5]*Department of Chemistry and Biochemistry, Eastern Washington University, Cheney, Washington 99004, USA*

(Received 4 March 2009; published 8 October 2009)

We investigated magnetoelastic coupling through the field-driven transition to the fully polarized magnetic state in quasi-two-dimensional $[Cu(HF_2)(pyz)_2]BF_4$ by magnetoinfrared spectroscopy. This transition modifies out-of-plane ring distortion and bending vibrational modes of the pyrazine ligand. The extent of these distortions increases with the field, systematically tracking the low-temperature magnetization. These distortions weaken the antiferromagnetic spin exchange, a finding that provides important insight into magnetic transitions in other copper halides.

DOI: 10.1103/PhysRevLett.103.157401 PACS numbers: 78.30.−j, 68.35.Ja, 75.30.Kz, 75.50.Ee

The interplay between structure and magnetism in correlated materials is an important factor leading to their complex properties, providing unique functionalities for fundamental physical property investigations and novel device applications. Magnetoelastic coupling effects associated with magnetic ordering transitions are commonly probed by x-ray, magnetostriction, heat capacity, dielectric constant, magnetization, and thermal conductivity [1–8]. These bulk measurements do not, however, provide information about the microscopic lattice response (e.g., local distortions that change site symmetry, bond lengths, and angles) coupled to a particular magnetic state. Instead, they provide information on average lattice behavior. To explore the microscopic lattice response, one must employ local probe techniques [9–16].

The detection of magnetoelastic coupling is most promising in antiferromagnetic (AFM) solids that reach magnetization saturation; i.e., all spin arrangements become ferromagnetic (FM), under moderate, experimentally realizable magnetic field. For such systems, AFM spin exchange interactions are generally weak. The magnetic exchange J between adjacent spin centers consists of a FM term J_F (≥ 0) and an AFM term J_{AF} (≤ 0), i.e., $J = J_F + J_{AF}$ [17]. The AFM term is related to the hopping integral t between spin sites as $J_{AF} = -4t^2/U$, where U is the effective on-site repulsion [17]. When an antiferromagnet is forced to adopt the FM state due to application of an external magnetic field, it can lower its energy by reducing the value of J_{AF}, i.e., by decreasing the hopping integral t. For a molecular AFM solid in which exchange takes place through a ligand, field-induced reduction of t may involve distortion of that molecular unit. Such symmetry breaking should be detectable by a local probe such as infrared spectroscopy.

As a candidate for a molecular solid with small J that can exhibit substantial magnetoelastic coupling, we consider the quasi–two-dimensional (2D) Heisenberg antiferromagnet $[Cu(HF_2)(pyz)_2]BF_4$. This compound consists of 2D square nets of Cu^{2+} ions [Fig. 1(a)] in which the intralayer AFM spin exchange between Cu^{2+} centers is mediated by pyrazine with $J = -6.1(3)$ K, and the interlayer FM spin exchange between Cu^{2+} ions by the HF_2^- bridging ligand with $J_\perp = 0.010(5)$ K [8,18–20]. Here, we employ a spin Hamiltonian of the form $-\sum J_{ij}\mathbf{S}_i \cdot \mathbf{S}_j$. Because of these overall low energy scales, a powered magnet can drive the system through the magnetic transition. $[Cu(HF_2)(pyz)_2]BF_4$ reaches the fully saturated state in an applied field of approximately 18 T at 500 mK and 1.5 K [8]. The sharp ''elbow'' denoting the critical field broadens at 4.2 K [8]. This is so because $T_N = 1.54$ K. Nevertheless, there is a strong similarity between the 4.2 and 1.5 K magnetization curves, demonstrating the well-

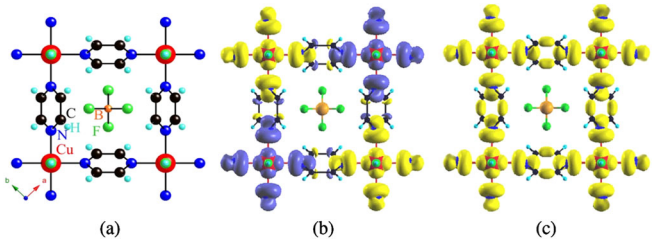

FIG. 1 (color online). (a) 300 K crystal structure of $[Cu(HF_2)(pyz)_2]BF_4$ [18]. This rendering emphasizes the quasi-two-dimensional nature of the Cu-pyrazine network. The bifluoride anions that link the Cu centers along c run into (and out of) the Letter. (b) and (c) Spin density distribution calculated for the AFM and FM state, respectively. Shading denotes different spins.

established fact that spin correlations in low-dimensional AFM materials are present well above the long-range magnetic ordering temperature [21]. These short range correlations are also manifested as a broad low-temperature maximum in the susceptibility [21,22].

Here, we investigate the field-induced transition to the fully polarized magnetic state in $[Cu(HF_2)(pyz)_2]BF_4$. We find that, in reaction to the change in state, the system lowers its magnetic exchange energy, in this case $|J_{AFM}|$, through magnetoelastic coupling. The beauty of the present experiment is that exchange is mediated by a molecular ligand, pyrazine, the value of the coupling being sensitively dependent on the geometry of the Cu-pyz-Cu path. Because the ligand is soft, it is easily distorted. We follow these local distortions by magnetoinfrared spectroscopy and demonstrate that they track the magnetic transition. This finding is relevant to field-driven magnetic ordering transitions in other low-dimensional quantum Heisenberg antiferromagnets such as the copper halides and complex materials with higher energy scales such as copper oxides, where AFM fluctuations of $S = 1/2$ centers may play a crucial role in establishing superconductivity but the size of the critical field precludes straightforward investigation of magnetostructural interactions [23]. These results are also important for understanding materials with more complicated noncollinear magnetic ordering transitions [13,24,25].

Single crystals were grown by solution techniques [26] and mixed with paraffin or KBr powder to form isotropic pellets for unpolarized transmittance measurements in the far and middle infrared, respectively [27]. Variable temperature studies were done at several temperatures between 300 and 4.2 K with 0.5 cm^{-1} resolution, and absorption was obtained as $\alpha(\omega) = -\frac{1}{hd}\ln\mathcal{T}(\omega)$, where h is the loading, d is the pellet thickness, and $\mathcal{T}(\omega)$ is the measured transmittance. Magnetoinfrared experiments were carried out at the NHMFL at 4.2 K using a 33 T resistive magnet. To emphasize field-induced changes in the optical properties, we calculated the absorption difference spectra $[\alpha(H) - \alpha(0\ T)]$. We quantify field-induced changes in the absolute absorption difference spectra as $\int_{\omega_i}^{\omega_f} |\alpha(H) - \alpha(0)| d\omega$, where ω_i and ω_f define the frequency range of interest. Spin density distributions for the AFM and FM states were calculated using the Vienna *ab initio* simulation package [28–30] with the generalized-gradient approximation [31], a 400 meV plane-wave cutoff energy, and 50 k points for the irreducible Brillouin zone. $U_{eff} = 4$ eV was employed for the Cu $3d$ states [32].

Figure 2 displays close-up views of several important infrared-active molecular vibrational modes in $[Cu(HF_2)(pyz)_2]BF_4$. Assignments were made using a combination of dynamics calculations, independent measurements on chemically similar model materials, and known functional group patterns [26]. Low-temperature mode splitting and redshifting were discussed extensively in Ref. [26] and attributed to a local structural distortion

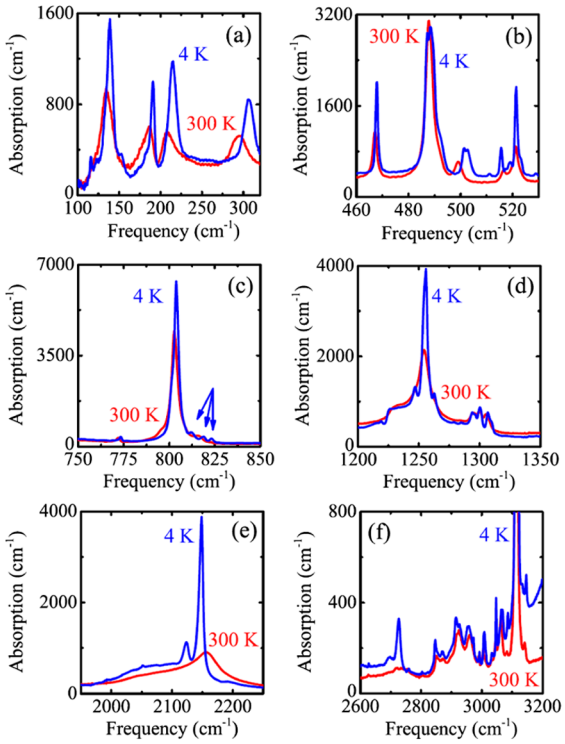

FIG. 2 (color online). Close-up views of selected vibrational modes in the absorption spectrum at 300 and 4 K. These include: (a) low frequency Cu-pyrazine lattice modes, (b) out-of-plane pyrazine ring deformation, out-of-plane pyrazine bend, and BF_4^- bend, (c) pyrazine out-of-plane C-H bend, (d) C-C stretch, (e) a combination-overtone mode, and (f) C-H stretching modes.

driven by improved low-temperature hydrogen bonding. The latter is evidenced by low-temperature redshifting of vibrational modes, an effect shown clearly in Fig. 2(e). This behavior is observed across the copper-pyrazine-based family of low-dimensional molecular magnets [33,34] and in related magnetic materials as well. A notable difference between these new measurements and the previous set is the presence of modest splitting in the Cu-pyrazine lattice mode centered at ~138 cm^{-1} at 4.2 K [Fig. 2(a)], indicative of a weak low-temperature distortion of the Cu^{2+} environment. Below, we focus on trends in the out-of-plane pyrazine ring deformation near 468 cm^{-1}, the out-of-plane pyrazine bend between 480 and 508 cm^{-1}, and the out-of-plane C-H bend of the pyrazine ring near 805 cm^{-1} [Figs. 2(b) and 2(c)]. These modes are molecular in nature.

Figure 3 displays the magnetoinfrared response of $[Cu(HF_2)(pyz)_2]BF_4$. Panels (a) and (b) show the absolute absorption in the two frequency regimes of interest: 450–510 cm^{-1} and 790–830 cm^{-1}. Field-induced spectral modifications are often difficult to see in $\alpha(\omega)$. As a consequence, we calculate absorption differences $[\alpha(H) - \alpha(0\ T)]$ to emphasize field-induced changes in the vibrational properties [Figs. 3(c) and 3(d)]. With increasing field, the out-of-plane pyrazine ring deformation, out-of-plane pyrazine bend, and pyrazine out-of-plane C-H bend-

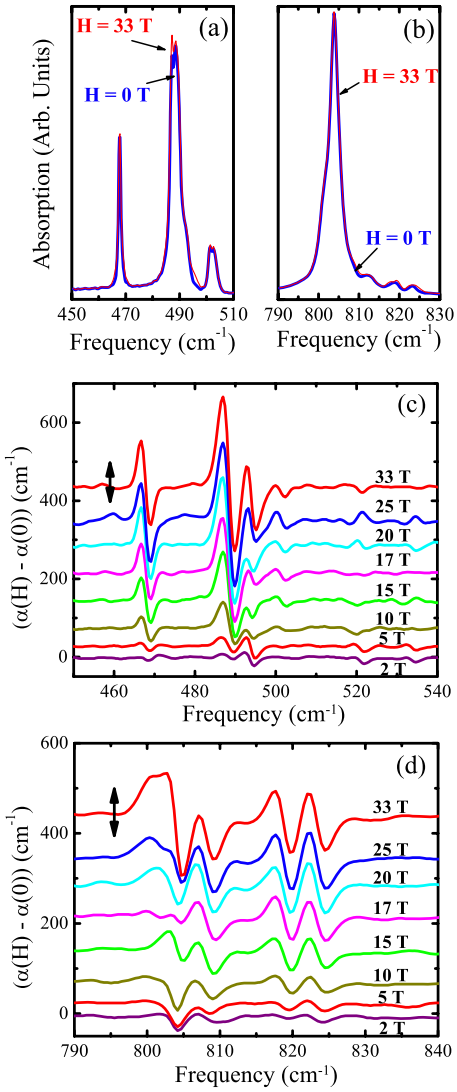

FIG. 3 (color online). (a) and (b) Close-up views of the absolute absorption spectra at $H = 0$ and 33 T at 4.2 K in the range of several pyrazine-related vibrational modes. (c) and (d) Close-up views of the 4.2 K absorption difference spectra $[\alpha(H) - \alpha(0\ \mathrm{T})]$ in the range of these same modes. Data in (c) and (d) are offset along the y axis for clarity. The double-headed arrows correspond to an absorption difference of 100 cm^{-1}. With this scale bar, we see that 33 T absorption differences near 490 cm^{-1} are on the order of 400 cm^{-1}. This corresponds to a 13% change in the out-of-plane pyrazine bending mode in a 33 T field.

ing modes redshift and increase slightly in intensity. The overall trend toward a softer lattice in applied magnetic field can be seen in the absolute absorption data [Figs. 3(a) and 3(b)], but it is more obvious in the absorption difference data where the characteristic derivativelike line shape is observed [Figs. 3(c) and 3(d)] [35]. Changes in the aforementioned ring-related modes are small but systematic at low fields, increase through H_c, and start to saturate above 25 T. At full field, the out-of-plane pyrazine ring deformation at 468 cm^{-1} displays an 11% change, the out-of-plane pyrazine bend at 488 cm^{-1} shows a 13% difference, the pyrazine out-of-plane C-H bend near 805 cm^{-1} has a 3.5% difference, and the small trio of peaks between 810 and 825 cm^{-1} change by about 30% at 33 T. In contrast, the frequency range (~515–520 cm^{-1}) where the BF_4^- mode resonates shows only fluctuations within our noise level, which is less than 0.05%. These results indicate that the field-driven transition to the fully polarized state is accompanied by strong changes in the out-of-plane pyrazine ring distortion and bending modes.

Before we discuss the consequences of out-of-plane pyrazine ring distortions for spin exchange interactions between Cu^{2+} centers, it is important to note that several characteristic vibrational modes of structurally important functional groups do not display any magnetic field dependence within our sensitivity. These include the Cu-pyrazine lattice modes, bifluoride linkers, and the BF_4^--related modes. That the BF_4^- bend near 520 cm^{-1} [Fig. 3(c)] is rigid is not such a surprise because it resides in the anion pocket without strong connectivity to the 2D spin exchange network. On the other hand, the low frequency Cu-pyrazine lattice modes and biflouride linkers are intimately involved in the 2D structural and magnetic framework and the interlayer connectivity and spin exchange interaction, respectively. From these spectral results, we see that the HF_2^- anion remains symmetric in the high field phase. Further, we find that interlayer magnetoelastic interactions as represented by the bifluoride group are unchanged in the fully polarized state. The behavior of the BF_4^- and HF_2^- molecular vibrations and the copper-pyrazine lattice modes clearly differs from that of the pyrazine ligands.

We can quantify trends in the out-of-plane pyrazine vibrations by integrating the absolute value of the absorption difference data and plotting the results as a function of field (Fig. 4). Here, integrations were carried out over two independent frequency regimes in order to follow the contrast in different modes. Strikingly, the spectral data track the magnetization, albeit with a small lag that may be

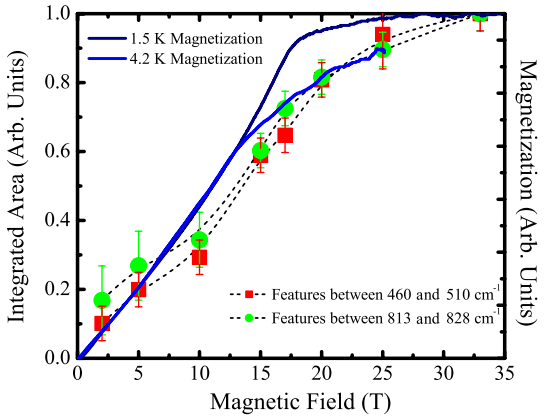

FIG. 4 (color online). Integrated area of the absolute value of the absorption difference spectra for the indicated frequency ranges as a function of applied magnetic field compared with 1.5 and 4.2 K magnetization data from Goddard *et al.* in Ref. [8]. The black dotted lines guide the eye.

related to slower lattice relaxation. That the size of these field-induced molecular-level distortions tracks the bulk magnetization demonstrates that the magnetoelastic interactions are coupled to the field-driven transition. This kind of coupling has not been observed before in any material to the best of our knowledge.

Magnetostructural correlations in chemically similar materials highlight the possible relationship between pyrazine ring tilt and magnetic exchange [8,36–39]. Considering this traditional interpretation and ring tilt data in $[Cu(HF_2)(pyz)_2]BF_4$ (31.6° away from c at 300 K, increasing at lower temperature), it is reasonable to anticipate field-driven orientational effects involving the pyrazine ligand. Instead, we found that the pyrazine ring distorts to accommodate the fully polarized magnetic state. Because the AFM term J_{AF} is determined by the overlap of the N lone pair orbitals of the pyrazine ring with the Cu x^2-y^2 orbital [Fig. 1(b)], the Cu-pyz-Cu spin exchange path is most effective when the twofold rotational axis coincides with the Cu-Cu direction and the pyrazine ring is planar. When the pyrazine ring is distorted from planarity, the hopping integral for the Cu-pyz-Cu spin exchange path becomes smaller, reducing the magnitude of J_{AF} as $-4t^2/U$. This reduces the overall spin exchange $J = J_F + J_{AF}$ since $J_F < |J_{AF}|$, effectively lowering the energy of the FM state forced upon the 2D antiferromagnet by external magnetic field. It is noted from Figs. 1(b) and 1(c) that the two C centers in each C-C bond of pyrazine have opposite spins in the AFM state but have identical spin polarizations in the FM state. The occurrence of an identical spin on both C centers weakens the C-C bond. This destabilizing effect in the FM state is reduced by the pyrazine out-of-plane distortion. It is also important to consider the role of lattice energy in the magnetoelastic effect. That this model 2D antiferromagnet is driven into the fully polarized state by an applied field demonstrates that the energy cost of distorting the pyrazine ring must be less than the magnetic energy gain in that state. Our preliminary density-functional calculations indicate that a 1° out-of-plane bend of the pyrazine ring can be accommodated in a 33 T field; such a hypothetical distortion changes J by $\sim$3%.

To summarize, we measured the vibrational properties of $[Cu(HF_2)(pyz)_2]BF_4$ through the magnetic field-driven transition to the fully polarized magnetic state in order to probe magnetoelastic coupling in a model 2D molecular antiferromagnet. The out-of-plane pyrazine ring deformation and bending modes redshift with applied field, and this contrast systematically tracks the low-temperature magnetization. The magnetoelastic coupling associated with this transition occurs most likely to reduce the strength of the Cu-pyz-Cu spin exchange in the FM state. Such a balance may be important in other magnetic materials.

This research was supported by the NSF (UT, NHMFL), the DoE (NHMFL, Argonne, NCSU), the Research Corporation (EWU), and the State of Florida (NHMFL). We thank P. A. Goddard for useful conversations and access to magnetization data. We thank J. S. Brooks and C. P. Landee for useful discussions.

[1] T. R. McGuire and W. A. Crapo, J. Appl. Phys. **33**, 1291 (1962).
[2] M. R. Ibarra *et al.*, Phys. Rev. Lett. **75**, 3541 (1995).
[3] S. J. Murray *et al.*, Appl. Phys. Lett. **77**, 886 (2000).
[4] A. N. Lavrov, S. Komiya, and Y. Ando, Nature (London) **418**, 385 (2002).
[5] M. Freamat *et al.*, Phys. Rev. B **72**, 014458 (2005).
[6] Y. Narumi *et al.*, J. Phys. Soc. Jpn. **75**, 075001 (2006).
[7] A. V. Sologubenko *et al.*, Phys. Rev. Lett. **98**, 107201 (2007).
[8] P. A. Goddard *et al.*, New J. Phys. **10**, 083025 (2008).
[9] T. Rudolf, Ch. Kant, F. Mayr, and A. Loidl, Phys. Rev. B **77**, 024421 (2008).
[10] R. Gupta *et al.*, Phys. Rev. Lett. **96**, 067004 (2006).
[11] C.-F. Sheu *et al.*, Inorg. Chem. **47**, 10 866 (2008).
[12] M. Sato and A. J. Sievers, Nature (London) **432**, 486 (2004).
[13] J. Cao *et al.*, Phys. Rev. Lett. **100**, 177205 (2008).
[14] J. Wong, *et al.*, Phys. Rev. B **30**, 5596 (1984).
[15] A. S. Masadeh *et al.*, Phys. Rev. B **76**, 115413 (2007).
[16] M. B. Smith *et al.*, J. Am. Chem. Soc. **130**, 6955 (2008).
[17] M.-H. Whangbo, H.-J. Koo, and D. Dai, J. Solid State Chem. **176**, 417 (2003).
[18] J. L. Manson *et al.*, Chem. Commun. (Cambridge) 47 (2006) 4894.
[19] M. Conner *et al.*, J. Low Temp. Phys. **142**, 273 (2006).
[20] P. Sengupta *et al.*, Phys. Rev. B **79**, 060409 (2009).
[21] L. J. de Jongh and A. R. Miedema, Adv. Phys. **23**, 1 (1974); **50**, 947 (2001).
[22] The broad maximum occurs at 5.5 K and is due to 2D AFM spin interactions within the layers. Our magneto-infrared data were obtained in the correlated regime below 5.5 K but slightly above T_N, where a strong remnant of the long-range ordered state still exists.
[23] J. Orenstein and A. J. Millis, Science **288**, 468 (2000), and references therein.
[24] P. A. Maggard *et al.*, Inorg. Chem. **41**, 4852 (2002).
[25] C. R. de la Cruz *et al.*, Phys. Rev. B **74**, 180402 (2006).
[26] S. Brown *et al.*, Inorg. Chem. **46**, 8577 (2007).
[27] High optical density precludes single crystal studies.
[28] P. E. Blöchl, Phys. Rev. B **50**, 17 953 (1994).
[29] G. Kresse and D. Joubert, Phys. Rev. B **59**, 1758 (1999).
[30] G. Kresse and J. Furthmüller, Phys. Rev. B **54**, 11 169 (1996).
[31] J. P. Perdew, K. Burke, and M. Ernzerhof, Phys. Rev. Lett. **77**, 3865 (1996).
[32] S. L. Dudarev *et al.*, Phys. Rev. B **57**, 1505 (1998).
[33] B. R. Jones *et al.*, Chem. Mater. **13**, 2127 (2001).
[34] J. Choi *et al.*, Chem. Mater. **15**, 2797 (2003).
[35] The redshift and softer lattice may be a signature of improved hydrogen bonding in the FM state [26].
[36] F. M. Woodward *et al.*, Phys. Rev. B **65**, 144412 (2002).
[37] C. P. Landee and M. M. Turnbull, Mol. Cryst. Liq. Cryst. **334**, 905 (1999).
[38] M. M. Turnbull and C. P. Landee, Mol. Cryst. Liq. Cryst. **334**, 957 (1999).
[39] P. R. Hammar *et al.*, Phys. Rev. B **59**, 1008 (1999).